Research on path navigation algorithm of garden robot based on Beidou and vision integration

Abstract:

In recent years, garden robots have gained increasing attention for their potential to automate tasks such as lawn maintenance, watering, and monitoring. However, a significant challenge in the development of these robots is achieving precise and reliable autonomous navigation in complex garden environments. This paper addresses this problem by proposing a combined navigation solution that integrates the Beidou satellite positioning system with a machine vision navigation system. The proposed approach aims to enhance the accuracy and robustness of garden robot navigation. The vision system employs an improved grayscale factor and vertical grayscale projection technique to filter out noise interference, leveraging differences in noise characteristics and road surface occupancy. Trapezoidal four-point coordinates are then used to extract the navigation path. For satellite-based positioning, the ultra-core HI600R module is utilized in conjunction with the HI600D reference station to construct a minimal RTK (Real-Time Kinematic) system. The raw data from both systems is processed using the Kalman filter algorithm, and the Gaussian-Krüger projection is applied to transform the coordinate system. The final navigation path is generated through a fusion algorithm that combines data from both the Beidou and vision systems. Experimental results demonstrate that the proposed navigation system achieves high accuracy and excellent stability, with an average positioning error of less than 0.2 meters in static conditions and less than 0.5 meters in dynamic conditions. These findings highlight the potential of the Beidou-vision fusion approach for practical applications in garden robot navigation.

Keywords: robotics, projection technology, noise filtering

1 Introduction

Autonomous navigation technology plays a crucial role in enabling vehicles to perceive their surroundings and autonomously plan travel paths. The core technologies underpinning this capability include positioning technology, environmental perception technology, and intelligent control technology [1]. In recent years, significant advancements have been made in these areas both domestically and internationally, yet challenges persist, particularly in achieving high precision and reliability in complex environments.

Global Navigation Satellite Systems (GNSS), such as the United States' GPS, Russia's GLONASS, and China's Beidou Navigation Satellite System, are widely used for positioning tasks [2]. Among these, the Beidou system has gained prominence due to its high accuracy, reliability, and growing global coverage. To meet the stringent requirements of autonomous navigation, centimeter-level positioning accuracy is essential. High-precision positioning technologies, such as Real-Time Kinematic (RTK) and Precise Point Positioning (PPP), have been developed to address this need [3]. While RTK offers real-time high-accuracy positioning, it requires a reference station, which can limit its application in certain scenarios.

Environmental perception technology relies heavily on sensors such as cameras, LiDAR, and radar to gather information about the surrounding environment. Vision-based systems, in particular, have been extensively studied due to their ability to detect obstacles, identify road

features, and provide detailed visual data [4]. Internationally, significant progress has been made in this field. For instance, American scholar E.R. Benson and colleagues proposed a machine vision guidance algorithm that accurately locates cut and uncut edges for agricultural machinery, providing lateral positioning signals for autonomous navigation [5]. Similarly, Vijay Subramanian and colleagues developed an integrated autonomous guidance system combining machine vision and LiDAR, demonstrating the potential of multi-sensor fusion approaches [6].

Despite these advancements, individual sensor technologies often face limitations. GNSS systems, for example, may suffer from signal loss or multipath interference in environments with dense vegetation or urban canyons. Vision-based systems, while powerful, can be affected by lighting conditions, weather, and occlusions. These limitations highlight the necessity for integrated navigation solutions that combine the strengths of multiple sensors to achieve robust performance.

Multi-sensor fusion-based integrated navigation technologies have emerged as a promising solution to overcome these challenges. However, existing research still faces gaps in terms of computational efficiency, data fusion accuracy, and adaptability to diverse environments. Specifically, the fusion of satellite-based positioning and vision-based perception remains an underexplored area, particularly in applications such as garden robots, where precise and reliable navigation is critical.

To address these issues, this paper proposes a novel navigation algorithm that integrates the Beidou satellite positioning system with a machine vision system. In the visual processing stage, an improved grayscale factor is introduced to enhance image preprocessing, followed by an edge extraction algorithm to optimize processing speed and accuracy. In the Beidou positioning stage, the Kalman filter algorithm is employed to refine raw positioning data, improving its precision and stability. Finally, the coordinate systems of the two subsystems are unified through Gaussian-Krüger projection, enabling seamless data fusion and generating a combined navigation path.

This approach aims to leverage the complementary strengths of Beidou and machine vision, addressing the limitations of individual sensors and advancing the state-of-the-art in autonomous navigation technology. By focusing on practical applications such as garden robots, the proposed solution seeks to bridge the gap between theoretical research and real-world implementation.

2. Machine Vision Algorithm

2.1 Experimental Platform Setup and Workflow

The experimental platform primarily consists of a tracked vehicle base, a main control computer, a camera, and a motor control module. The camera used is the HQ-USB-1080HD camera module from LeGo Intelligent Electronics, which utilizes USB 2.0 for data transmission. Experimental data is processed using the MATLAB platform.

2.2 Image Preprocessing

2.2.1 Image Cropping

Since structured garden roads are the main focus of this study, and garden roads typically feature relatively straight lines on both sides with some curvatures in certain areas, part of the image is cropped. This reduces interference, simplifies the computational load, and improves image processing speed, while also addressing the curvature issues of winding roads [7]. After conducting multiple experiments, it was determined that cropping the lower 300 rows of the

captured image yielded the best results.

2.2.2 Grayscale Conversion

Common methods for image grayscale conversion include the component method, maximum value method, average value method, and weighted average method [8]. Considering that the vehicle operates in garden road environments, the super-green feature threshold segmentation algorithm is typically employed. This algorithm effectively suppresses interference from shadows, dry grass, and road surfaces, thereby highlighting plant and grass images and enabling more effective extraction of green vegetation images [9]. The super-green feature threshold segmentation factor is defined as shown in Equation (1). Based on this factor, this paper proposes an improved grayscale factor, as expressed in Equation (2). In the equations, gray(x,y) epresents the grayscaled image, while R, G, and B denote the red, green, and blue color components of the original color image, respectively.

$$\mathrm{gray}(x,y) = \begin{cases} 0, & 2G - R - B < 0 \\ 255, & 2G - R - B > 255 \\ 2G(x,y) - R(x,y) - B(x,y), & \text{else} \end{cases} \quad (1)$$

$$\mathrm{gray}(x,y) = \begin{cases} 0, & 3R - 2B - G < 0 \\ 255, & 3R - 2B - G > 255 \\ 2B(x,y) - G(x,y), & \text{else} \end{cases} \quad (2)$$

This study adopts a method of first cropping the original image and then applying grayscale conversion. This approach reduces the pixel size of the image and decreases the number of pixels to be processed, thereby not only improving the algorithm's operational speed but also enhancing the overall robustness of the system. The effectiveness of the proposed new grayscale factor was validated through 100 sets of comparative experiments, as shown in Figure 1:

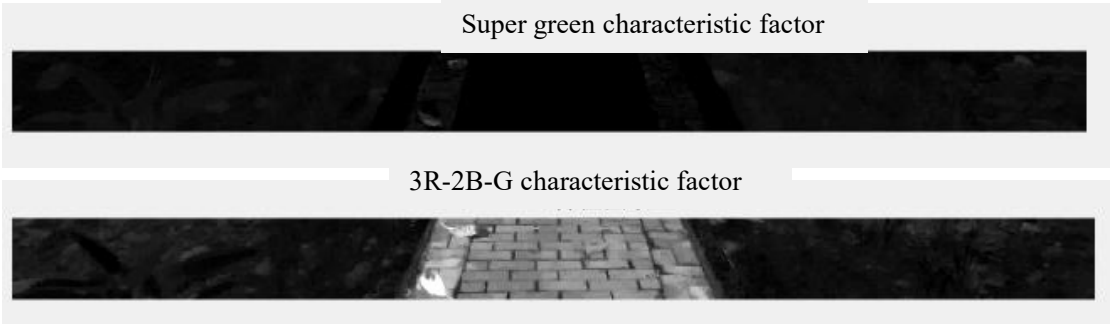

Figure 1 Comparison of Experimental Results

As shown in Figure 1, the improved grayscale factor demonstrates a significantly better suppression effect on road surface pixels in garden environments compared to the super-green feature factor. It also provides more prominent segmentation of edge pixels.

2.2.3 Image Filtering and Binarization

Considering the working environment of the robot, salt-and-pepper noise was intentionally added to the images, and median filtering was applied for smoothing. Image binarization is a critical method in machine vision for segmenting images. Its principle involves setting the grayscale values of the pixels in the image to either 0 or 255. Common binarization methods include Otsu's method (maximum between-class variance), maximum entropy thresholding, the bimodal method, and the iterative method (optimal thresholding) [10]. In this study, Otsu's method

was used for image binarization. Otsu's method is an algorithm that determines the optimal threshold for binarization by maximizing the between-class variance of the foreground and background in an image. Considering the complexity of the robot's operational environment, the threshold obtained using Otsu's method was applied for binarization, ensuring that the variance between the foreground and background classes was maximized.

2.2.4 Mathematical Morphology Processing

Morphological processing typically involves the use of opening or closing operations. Opening operations are primarily used to eliminate small regions with high brightness, while closing operations are mainly used to fill in small holes [11]. After image binarization, noise and small holes are often present. To eliminate these interferences, morphological closing operations can be applied to fill in the holes, as expressed in Equation (3).

$$A \cdot B = （A \oplus B） \ominus B \quad (3)$$

In this context, A represents the image, and B is the structuring element. The morphological closing operation involves first dilating image A with structuring element B, as expressed in Equation (4), and then eroding the resulting image C with , as expressed in Equation (5).

$$A \oplus B = \{x|(B + x) \cap x \neq \emptyset\} \quad (4)$$

$$C \ominus B = \{x|(B + x) \subseteq A\} \quad (5)$$

2.3 Navigation Line Extraction

2.3.1 Vertical Grayscale Projection

According to the principles of camera imaging, road images in the surface region are approximately trapezoidal. Therefore, the key to extracting navigation lines lies in detecting the road edges and segmenting the road from the background [12]. Commonly used edge detection operators include the Roberts operator, Prewitt operator, Sobel operator, Laplacian operator, and Canny operator [13]. However, these differential operators require derivative calculations, which increase the processing time for the computer.

This study employs the vertical grayscale projection method of pixel points to obtain the road surface region. Based on the significant size difference between noise and the road surface region, an appropriate threshold is selected to eliminate the influence of noise. The specific process is as follows:

1) In the binary image, white pixel points correspond to a pixel value of 1, and black pixel points correspond to a pixel value of 0. The pixel values in each column are then summed, as shown in Equation (6).

$$V(i,j) = \sum_{i=1}^{n} A(i,j), j = 0,1,2,\cdots,m \quad (6)$$

In this equation, V(i,j) represents the sum of the pixel values in each column, A(i,j) is the value of each pixel in the binary image, n is the total number of columns in the binary image, and m is the total number of rows in the binary image.

2) An appropriate threshold T is selected, and regions in V(i,j) with values less than T are identified as noise. The values in these regions are then set to 0.

3) The column coordinates corresponding to the maximum values in V(i,j) are taken as the upper vertex coordinates X_1 and X_2 of the trapezoid, while the column coordinates corresponding to the minimum values are taken as the lower vertex coordinates X_3 and X_4.

2.3.2 Navigation Line Extraction

Currently, navigation line extraction is commonly performed using the Hough transform or the least squares method [14]. The least squares method is prone to interference from noise points

[15], while the Hough transform, although resistant to noise, has high time and space complexity due to its inherent characteristics [16]. Considering these factors, this study leverages the specific properties of camera imaging, where the road region image is approximately trapezoidal, and uses the four vertices of the extracted trapezoid to determine the navigation line.

Based on the geometric properties of the trapezoid, the axis line corresponds to the robot's travel path. The midpoints of the upper and lower bases of the trapezoid can be calculated using Equations (7) and (8), and the navigation line can be obtained using the two-point form of a straight line as expressed in Equation (9).

$$C_1 = \frac{X_1+X_2}{2} \quad (7)$$

$$C_2 = \frac{X_3+X_4}{2} \quad (8)$$

$$\frac{y-y_2}{y_1-y_2} = \frac{x-x_2}{x_1-x_2} \quad (9)$$

In this context, C_1 and C_2 represent the midpoint coordinates of the upper and lower bases, respectively. (x_1,y_1) are the coordinates of point C_1, and (x_2,y_2) are the coordinates of point C_2.

2.4 Experiment and Analysis

The experiment was conducted at Nanning Flower Park, with image capture sizes of 480×640. To verify the effectiveness of the proposed algorithm, a relatively complex image was selected as the research object. The original image is shown in Figure 2(a); the cropped image containing the valid region of the last 300 rows is shown in Figure 2(b); the grayscale image obtained using the super-green feature factor for grayscale processing is shown in Figure 2(c); the grayscale image obtained using the improved feature factor for grayscale processing is shown in Figure 2(d); after applying Otsu's method for binarization to Figure 2(d), the result is shown in Figure 2(e). As can be seen, there is still a significant amount of noise interference, but performing a morphological closing operation eliminates most of the noise, as shown in Figure 2(f); the vertical grayscale projection of Figure 2(f) is shown in Figure 2(g); after selecting threshold T to eliminate noise, the result is shown in Figure 2(h); after extracting the midpoint coordinates using the proposed algorithm, the connected navigation line is shown in Figure 2(i); and finally, the fitted robot travel path is shown in Figure 2(j).

(a) Original Image

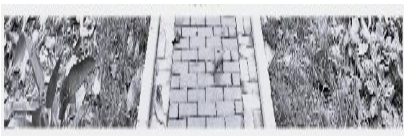

(b) Cropped Image

(c) Super-Green Feature Factor

(d) Improved Grayscale Factor

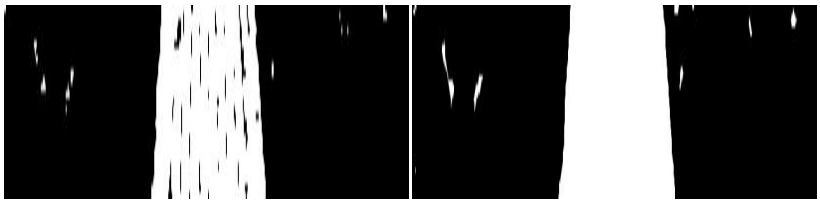

(e) Binarization (f) Mathematical Morphological Processing

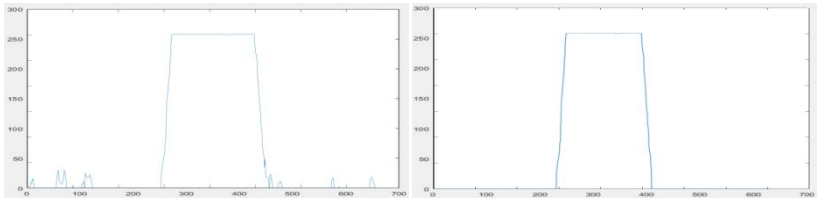

(g) Vertical Grayscale Projection (h) After Noise Elimination

(i) Extracted Navigation Line (j) Fitted Navigation Line

Figure 2 Experimental Processing Images

3 Beidou Navigation-Based Positioning Algorithm

3.1 Beidou Navigation Satellite System

The Beidou Navigation Satellite System (BDS) is an independently developed satellite navigation system by China, and it is the third mature satellite navigation system after the GPS (Global Positioning System) developed by the United States and the GLONASS (Glonass System) developed by Russia. In the late 20th century, due to the needs of national security and economic and social development, China began to gradually build a global satellite navigation system. This system provides global users with all-weather, all-time, high-precision positioning, navigation, and timing services, and serves as an essential space-time infrastructure for the country.

3.1.1 Composition of the Beidou System

The GNSS (Global Navigation Satellite System) refers to a global navigation satellite system that uses artificial satellites as navigation stations in a stellar radio navigation system. The Beidou system is a typical example of a GNSS positioning system [19].

As shown in Figure 3, the BDS primarily consists of a ground control segment, a space segment, and a user terminal segment.

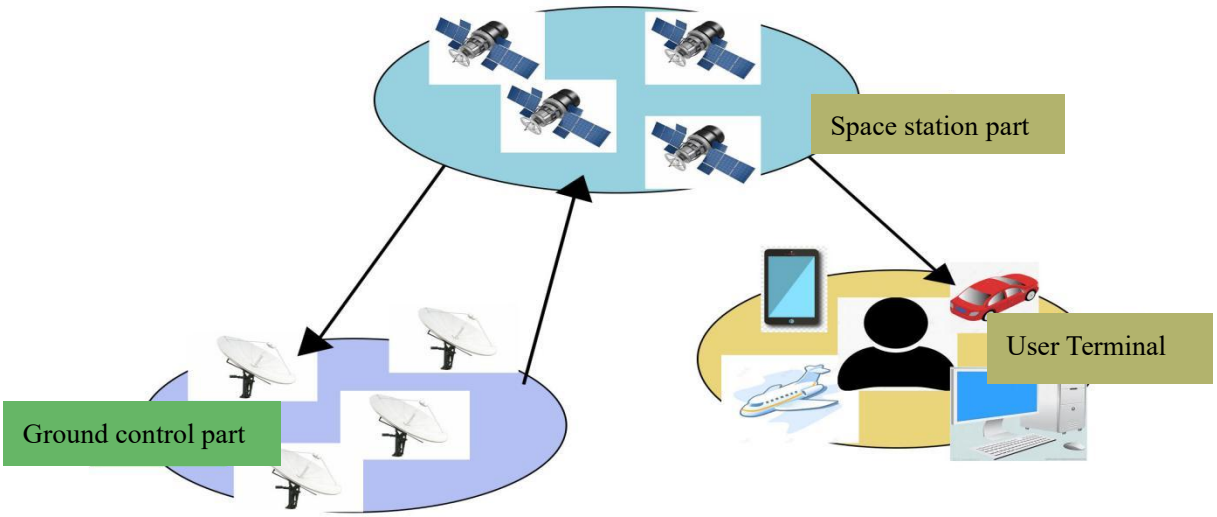

Figure 3 The Composition of the Beidou Navigation Satellite System

(1) Space Segment

Since the intensive launch of Beidou-3 satellites started in 2017, the space segment of Beidou-3 consists of 30 satellites. This includes 3 geostationary orbit (GEO) satellites, 24 medium earth orbit (MEO) satellites, and 3 inclined geosynchronous orbit (IGSO) satellites [20].

(2) Ground Control Segment

The ground control segment is composed of the main control station, time-space synchronization injection stations, and monitoring stations. The main control station is responsible for the operation management and control of the system. It collects observational data from various monitoring stations, processes it to generate wide-area differential information, integrity information, and satellite navigation messages, and then instructs the injection stations to transmit the information. The injection stations' function is to transmit signals to the satellites, manage and control the satellites, and after receiving instructions from the main control station, relay the information to the satellites. The monitoring stations' function is to continuously track and monitor the navigation satellites in real time, determine their orbits, receive signals from the satellites, and send them to the main control station. They also provide observation data for time synchronization [21].

(3) User Terminal Segment

The user terminal segment refers to the terminal users of the Beidou Navigation System, other compatible terminal users of different navigation systems, and the related application service systems. Currently, the Beidou-3 system provides a variety of services, including navigation, positioning, timing, short message communication, satellite-based augmentation, ground-based augmentation, international search and rescue, and precise point positioning. The global positioning accuracy is better than 10 meters, timing accuracy is better than 20 nanoseconds, speed measurement accuracy is better than 0.2 meters/second, and the global service availability exceeds 99%. Furthermore, its performance is better in the Asia-Pacific region [22].

3.1.2 Positioning Principle of the Beidou System

The positioning principle of the Beidou Satellite Navigation System is based on the trilateration measurement method. The core idea of this method is to determine the position of a target point using the positional information of three spheres. Specifically, three satellites serve as the centers of the spheres, and the distances from these satellites to the user receiver are used as the radii. These three spheres will intersect at two points. Assuming the coordinates of the three satellites are known as A, B, and C, the distances from the satellites to the user receiver are r1, r2, and r3, respectively, and the coordinates of the user receiver are denoted as P. The following equations can then be established, as shown in Equation 10:

$$\begin{cases} R_1^2 = (X_1 - X_u)^2 + (Y_1 - Y_u)^2 + (Z_1 - Z_u)^2 \\ R_2^2 = (X_2 - X_u)^2 + (Y_2 - Y_u)^2 + (Z_2 - Z_u)^2 \\ R_3^2 = (X_3 - X_u)^2 + (Y_3 - Y_u)^2 + (Z_3 - Z_u)^2 \end{cases} \quad (10)$$

The distance R from the satellite to the user receiver can be calculated based on the propagation speed of radio waves in the atmosphere, denoted as c, and the time taken for the radio wave to travel from transmission to reception, as shown in Equation 11:

$$\mathrm{R_i} = \mathrm{c} \cdot \Delta \mathrm{t} \ , \ \mathrm{i} = 1,2,3 \quad (11)$$

Using Equations (10) and (11), the coordinates of the two intersection points can be determined. Based on engineering experience, the point that does not coincide with the Earth's surface can be easily excluded. The remaining point is the true position of the user receiver. This forms the fundamental principle of the Beidou positioning system. However, in practical calculations, factors such as satellite clock errors must also be considered. Therefore, the positional information of an additional satellite is required to further complete the position calculation.

3.2 NMEA-0183 Communication Protocol

NMEA stands for the National Marine Electronics Association in the United States. The NMEA-0183 protocol is currently the most widely used protocol in satellite positioning receivers. The NMEA-0183 protocol is based on ASCII code and defines numerous sentences. Among these, the most commonly used and widely compatible ones include GGA (Global Positioning System Fix Data) for GPS positioning information, RMC (Recommended Minimum Specific GPS/TRANSIT Data) for recommended positioning information, and VTG (Track Made Good and Ground Speed) for ground speed information [23]. Taking "RMC" data as an example, its specific format and details are as follows:

$GPRMC,020550.c00,A,2813.9891299,N,11252.6278784,E,0.033,315.7,161117,0.0,E,A*30

The specific format and explanation are shown in Table 1:

Table 1: Explanation of Positioning Information Data Sentences

ID	Example	Description
1	$GPRMC	Start symbol + message type
2	020550.00	UTC time
3	A	Positioning status: A – valid positioning, V – invalid positioning
4	2813.9891299	Latitude: 28°13.99891299', with the range of 0° to 90°. The integer part represents minutes, and the remaining part represents degrees.
5	N	Latitude direction: N – North, S – South
6	11252.6278784	Longitude: 112°52.6278784', with the range of 0° to 180°. The integer part represents minutes, and the remaining part represents degrees.
7	E	Longitude direction: E – East, W – West

8	0.033	Ground speed, unit: knots (N)
9	315.7	Ground course, with true north as the reference, the angle in the clockwise direction to the course. (Range: 0° ~ 360°)
10	161117	Date: day, month, year
11	0.0	Magnetic declination, unit: degrees
12	E	Magnetic declination direction
13	A	Mode indication: N = data invalid; A = autonomous positioning; E = estimated; D = differential; M = manual input
14	30	Checksum

3.3 Kalman Filtering Algorithm

Kalman filtering is an algorithm that provides an optimal estimate of the system state based on the state-space representation of a linear system, using system inputs and output observation data [24]. Kalman filtering does not require the assumption that both the signal and noise are stationary. As long as the measurement variance is known, it can process a series of noisy observations and provide an estimate of the true signal with minimal error. Kalman filtering is a recursive process that continuously updates and corrects the data during operation. It does not require storing large amounts of observed data. During its calculation, it only needs the previous estimate and the most recent observation value to predict the current state, allowing for real-time state estimation with fast response times. Therefore, Kalman filtering is widely used in the dynamic data processing of GPS and Beidou satellite positioning. When control input is not considered, the system model is as shown in Equation (12):

$$\begin{cases} X_k = AX_{k-1} + W_{k-1} \\ \mathrm{Z_k} = \mathrm{HX_k} + \mathrm{V_k} \end{cases} \quad (12)$$

In Equation (12), X is the system state vector, Z is the observation vector, A is the state transition matrix, and H is the observation matrix. W and V represent the process noise and measurement noise, respectively, with covariance matrices Q and R, both of which are zero-mean white noise, as shown in Equation (13):

$$\begin{cases} \mathrm{E(W_k)} = 0, \mathrm{COV(W_k)} = \mathrm{E(W_k W_k^T)} = \mathrm{Q} \\ \mathrm{E(V_k)} = 0, \mathrm{COV(V_k)} = \mathrm{E(V_k V_k^T)} = \mathrm{R} \end{cases} \quad (13)$$

The recursive process is as follows:

State prediction process:

$$\begin{cases} \widehat{X_{\bar{k}}} = A\widehat{X_{k-1}} \\ P_{\bar{k}} = AP_kA^T + Q \end{cases} \quad (14)$$

Measurement update process:

$$\begin{cases} K_k = P_{\bar{k}}H^T(HP_{\bar{k}}H^T + R)^{-1} \\ \widehat{X_k} = \widehat{X_{\bar{k}}} + K_k(Z_k - H\widehat{X_{\bar{k}}}) \\ P_k = (I - K_kH)P_{\bar{k}} \end{cases} \quad (15)$$

Where X_k represents the posterior state estimate at time k, X_{k-1} represents the prior state estimate at time k, P_k represents the posterior estimate covariance at time k, P_{k-1} represents the prior estimate covariance at time k, and K_k represents the Kalman gain.

3.4 Semi-Physical Simulation Analysis Based on Kalman Filtering

3.4.1 Building the RTK System

RTK (Real-Time Kinematic) technology achieves centimeter-level high-precision positioning through differential correction messages (RTCM) broadcast by the reference station [25]. The reference station receiver broadcasts differential data (including the type, location, and observation data of the reference station receiver), while the rover station receiver receives the differential data and satellite signals in real-time for calculation. When the rover station receiver eliminates the errors in the observation data and "fixes" the integer number of carrier phase observations, obtaining centimeter-level position information, the RTK fixed solution is achieved.

Firstly, two Beidou modules are used with RTK (Real-Time Kinematic) technology to obtain high-precision positioning, and the obtained data is set as the true value. The HI600D is used as the reference station, and the HI600R as the rover station, thus building a minimal RTK system. Both modules are connected to a computer, with the rover station's positioning module outputting RTK results. The serial port debugging software is used to read and save the data. The connection is shown in Figure 4 below:

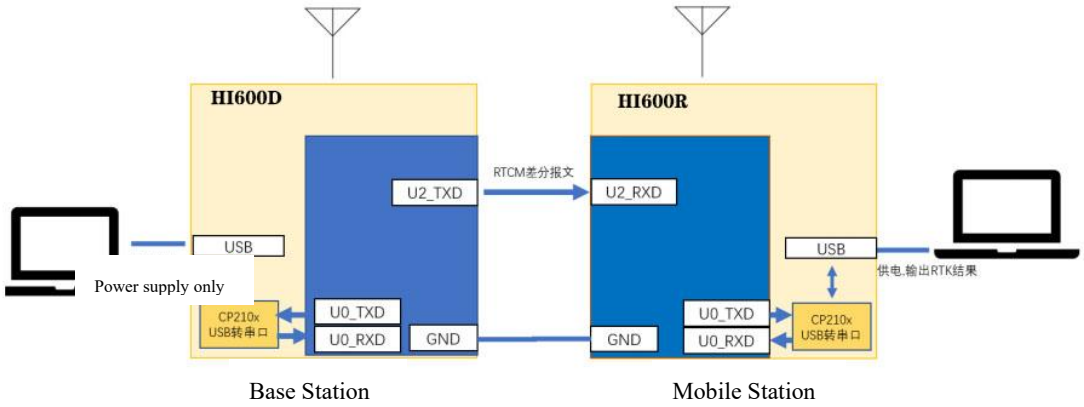

Figure 4: Minimal RTK System

3.4.2 Semi-Physical Simulation Analysis

The simulation analysis is divided into two groups: one for static data and one for dynamic data. In the static data group, the data obtained using RTK technology is set as the true value. The simulation time Latitude Tracking with a sampling interval of 1 second, and the true system values are [24.3055565; 109.3724454]. The Kalman filtering algorithm is used to filter the original Beidou positioning observation data. Figure 5(a) shows the comparison of the latitude position variation of the static object obtained using Kalman filtering with the original and true data. Figure 5(b) shows the comparison of the longitude position variation of the static object obtained using Kalman filtering with the original and true data. In the dynamic data group, the simulation time is 450 seconds with a sampling interval of 1 second. Figure 6(a) shows the comparison of the latitude position variation of the dynamic object obtained using Kalman filtering with the original data. Figure 6(b) shows the comparison of the longitude position variation of the dynamic object obtained using Kalman filtering with the original data.

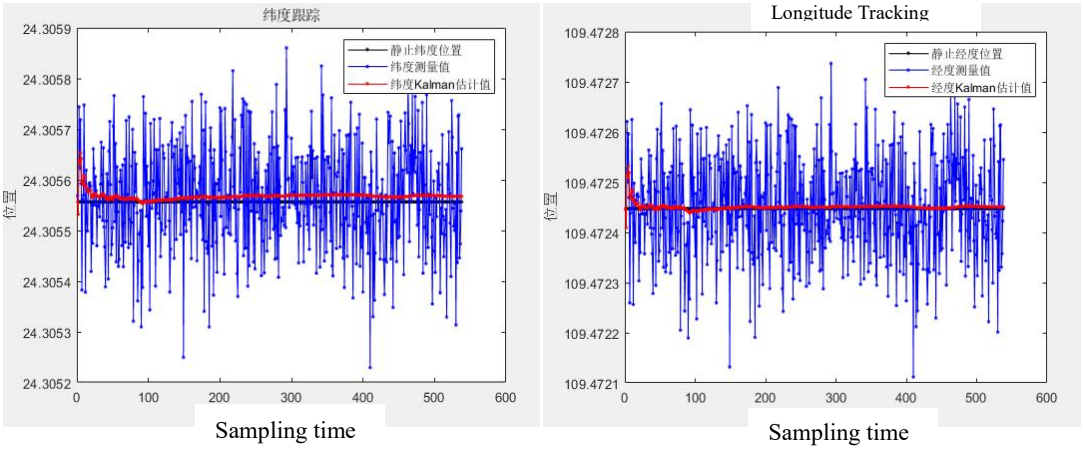

Figure 5: Comparison of Static Kalman Filtering with Original and True Data

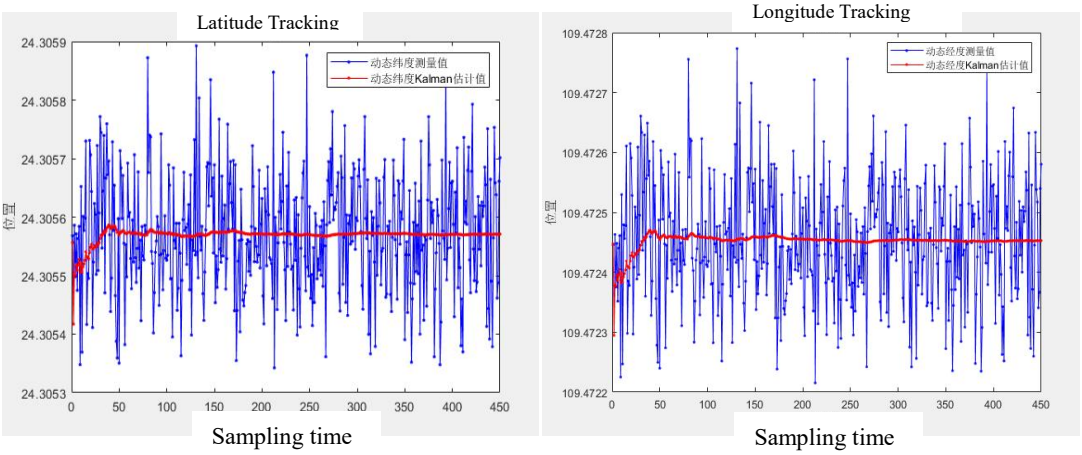

Figure 6: Comparison of Dynamic Kalman Filtering with Original and True Data

From the simulation results, in the static data, the positioning data processed by Kalman filtering is noticeably smoother than the original measurement data, converging more quickly and getting closer to the true values obtained using the RTK algorithm. In the dynamic data, the data processed by Kalman filtering also shows significantly less fluctuation compared to the original data. The simulation analysis results show that the Kalman filtering method can effectively improve the positioning accuracy and convergence speed.

4. Study of Combined Positioning Algorithm Based on Beidou and Vision Systems

In general, combined navigation technology typically refers to the use of two or more navigation systems with complementary measurement advantages to measure the same information source and achieve higher navigation accuracy. One navigation system usually provides short-term, high-precision information, while the other provides long-term, high-stability information. Compared to a single navigation system, the combined navigation system offers greater advantages in navigation accuracy.

4.1 Research on Multi-Sensor Information Data Fusion Technology

Multi-sensor fusion technology refers to the analysis, estimation, and integration of information and data from multiple sensors or signal sources using specific data fusion algorithms, in order to make the required decisions and estimates. Multi-sensor fusion technology combines and optimizes the information obtained by various sensors about the same target features through multi-level and multi-space complementary processing, ultimately generating reliable information

about the observed target features [26]. The general structure of multi-sensor information data fusion is shown in Figure 7.

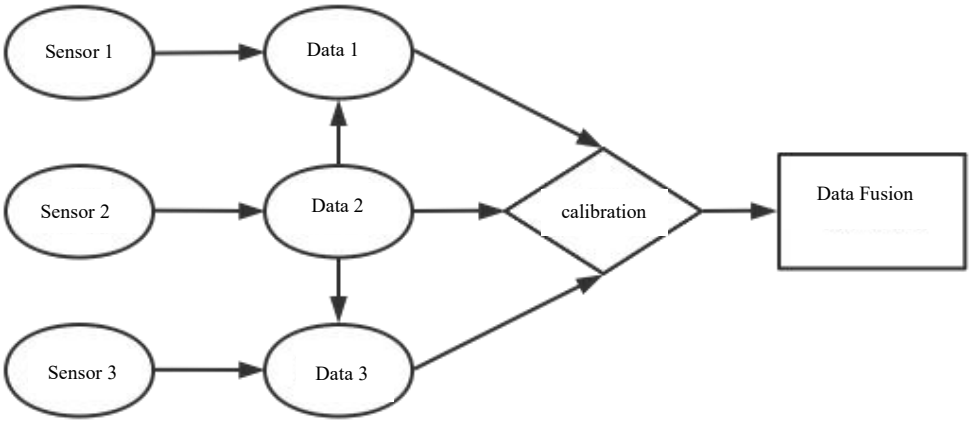

Figure 7: Multi-Sensor Information Fusion Structure

4.2 Common Algorithms for Data Fusion Technology

For multi-sensor systems, due to the diversity and complexity of information, the basic requirements for information fusion algorithms are their robustness and parallel processing capability. Other requirements include algorithm speed and accuracy. In general, nonlinear mathematical methods that have fault tolerance, adaptability, associative memory, and parallel processing ability can all be used as fusion methods [27]. The following are several commonly used data fusion algorithms:

(1) Weighted Averaging Method

The weighted averaging method is the simplest and most intuitive method in signal-level fusion. The specific approach is to take the data collected by a set of sensors and compute a weighted average, using the result of the weighted average as the final output fusion value. This method directly operates on the data sources.

(2) Kalman Filtering Method

This method is mainly used to fuse redundant data from low-level real-time dynamic multi-sensors. It uses the statistical characteristics of the measurement model to recursively determine the optimal fusion and data estimation in a statistical sense. If the system has a linear dynamic model, and the errors of the system and sensors follow a Gaussian white noise model, Kalman filtering will provide the unique optimal estimation for fused data in a statistical sense. The recursive nature of Kalman filtering allows the system to process data without requiring large amounts of data storage and computation.

(3) Multi-Bayesian Estimation Method

Each sensor is treated as a Bayesian estimator, and the individual objects' associated probability distributions are combined into a joint posterior probability distribution function. By minimizing the likelihood function of the joint distribution function, the final fused value of multi-sensor information is provided. The fused information, along with a prior model of the environment, is used to provide a feature description of the entire environment.

(4) Artificial Neural Network Method

Neural networks have strong fault tolerance, self-learning, self-organization, and self-adaptive capabilities, and can simulate complex nonlinear mappings. These characteristics, along with their powerful nonlinear processing capabilities, make neural networks well-suited to meet the requirements of multi-sensor data fusion technology. In a multi-sensor system, the environmental information provided by each information source has a certain degree of uncertainty. The fusion process of these uncertain pieces of information is essentially an uncertain reasoning process. Neural networks determine classification standards based on the similarity of the samples received by the current system. This determination method is mainly reflected in the network's weight distribution. Learning algorithms can also be used to acquire knowledge, forming an uncertainty reasoning mechanism. By utilizing the signal processing capability and automatic reasoning function of neural networks, multi-sensor data fusion can be achieved.

4.3 Overall Design of the Integrated Navigation System

There are many types of integrated navigation methods, such as the typical combination of inertial navigation and GPS (INS/GPS), GPS and LiDAR integration, GPS and vision integration, etc. By leveraging the joint perception of multiple sensors, integrated navigation systems can provide more accurate position or velocity information, enhanced reliability, and lower costs compared to traditional single-sensor navigation systems. As a result, they are gaining increasing popularity across various fields. This paper adopts a combination of machine vision and BDS navigation, analyzing the advantages and disadvantages of using these two navigation methods. The integrated navigation system, compared to the original single-system navigation, shows significant improvements in stability, accuracy, and performance. The overall design is shown in Figure 8.

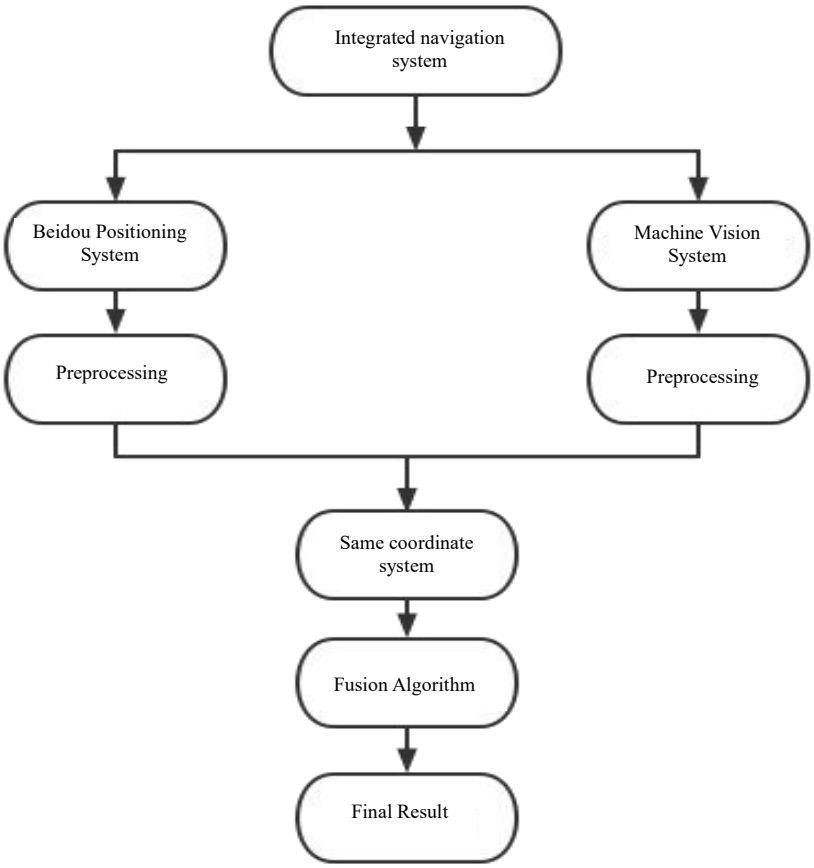

Figure 8: Overall Structure of the Integrated Navigation System

4.4 Data Calibration for Integrated Navigation System

4.4.1 Gauss-Krüger Projection

Since BDS uses a three-dimensional Beidou coordinate system, directly utilizing this coordinate system is not conducive to the subsequent design of the navigation system. Therefore, the Gauss-Krüger projection method is employed for coordinate system transformation. The Gauss-Krüger projection is a conformal projection between the Earth's ellipsoid and a plane. The basic concept is as follows: A cylindrical projection is tangent to a meridian on the Earth's ellipsoid, with the central axis of the cylindrical projection coinciding with the equatorial plane. The Earth's ellipsoid is conditionally projected onto the cylindrical surface of the ellipsoid. As shown in Figure 9.

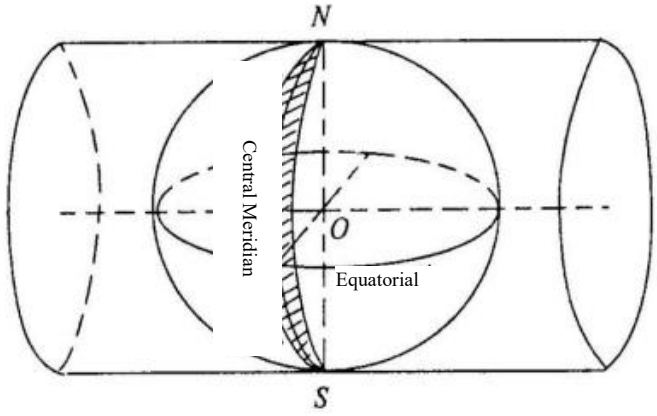

Figure 9: Gauss Projection Diagram

The characteristic of the Gauss projection is that there is no angular distortion, and the shape changes are minimal. The central meridian does not cause any distortion, but the further away from the central meridian, the greater the distortion. To limit this distortion, the Gauss-Krüger projection method employs a zonal projection. Zonal projections are divided into 3° and 6° bands, where the central meridian is used as the starting point, and each band is numbered sequentially with a fixed longitudinal difference from west to east, as shown in Figure 10.

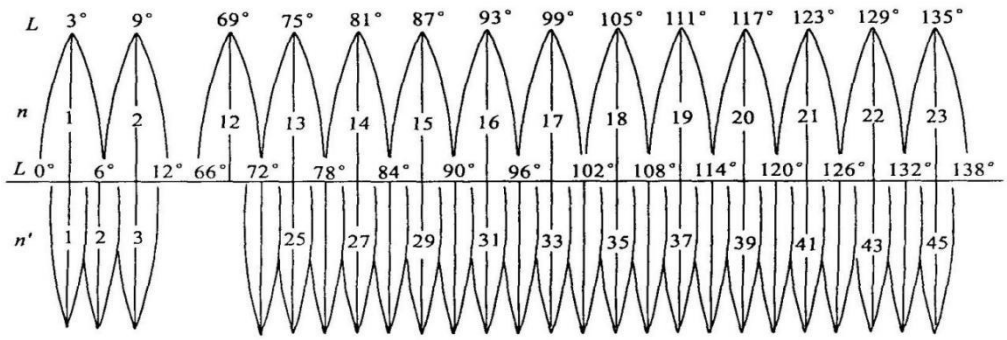

Figure 10. Schematic diagram of projection zone division.

The current zone can be determined based on the known longitude. For example, the longitude of Guangxi University is approximately 108.29°, which places it in Zone 19 when divided by 6° bands and in Zone 36 when divided by 3° bands. Given the known latitude and longitude coordinates (L, B), the coordinates (x, y) in the Gauss plane rectangular coordinate system can be calculated using the direct Gauss projection formula (16).

$$\begin{cases} x = X + \dfrac{N}{2\rho''^2}\sin B\cos B\cdot l''^2 + \dfrac{N}{24\rho''^4}\sin B\cos^3 B\,(5 - t^2 + 9\eta^2 + 4\eta^4)\,l''^4 \\ \qquad + \dfrac{N}{720\rho''^6}\sin B\cos^5 B\,(61 - 58t^2 + t^4)l''^6 \\ y = \dfrac{N}{\rho''}\cos B\cdot l'' + \dfrac{N}{6\rho''^3}\cos^3 B\,(1 - t^2 + \eta^2)l''^3 + \\ + \dfrac{N}{120\rho''^5}\cos^5 B\,(5 - 18t^2 + t^4 + 14\eta^2 - 58\eta^2 t^2)l''^5 \end{cases} \tag{16}$$

In the formula: $l'' = \mathrm{L} - \mathrm{L}_0$, L_0 is the central meridian longitude; $\mathrm{N} = \mathrm{a}(1 - \mathrm{e}^2\sin^2\mathrm{B})^{-\frac{1}{2}}$, N is the

radius of curvature in the meridian plane, a is the length of the Earth's ellipsoid semi-major axis, and e is the first eccentricity of the ellipsoid; $t = \tan B$, $\eta^2 = e'^2 \cos^2 B$, $\rho'' = \frac{180}{\pi} * 3600$, e'is the second eccentricity of the Earth; X is the meridian arc length, which can be calculated using a practical formula $X = 111132.9525B - 16038.5087 \sin 2B + 16.8326 \sin 4B - 0.022 \sin 6B$ calculated.

Figure 11 shows the latitude and longitude coordinates obtained directly from BDS based on the Beidou coordinate system, while Figure 12 shows the positioning information in the Gauss plane coordinate system after Gauss projection.

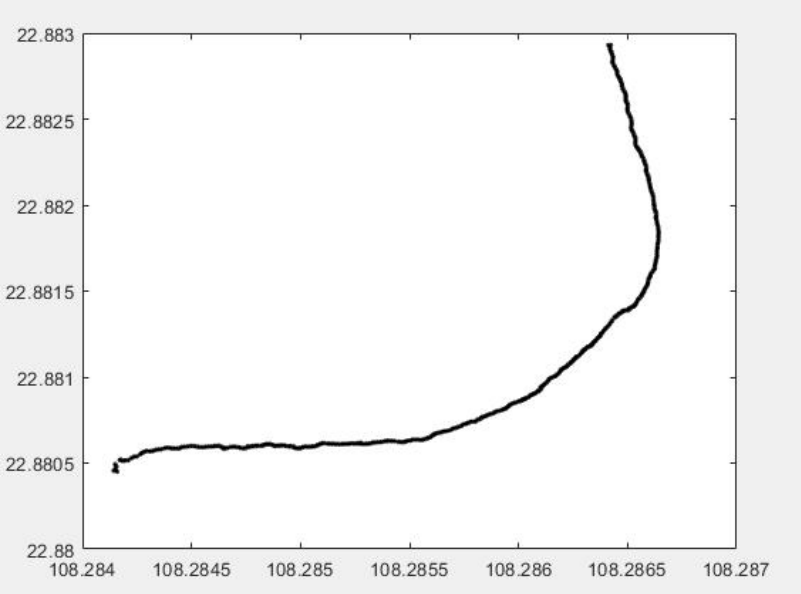

Figure 11. Latitude and longitude information in the Beidou coordinate system.

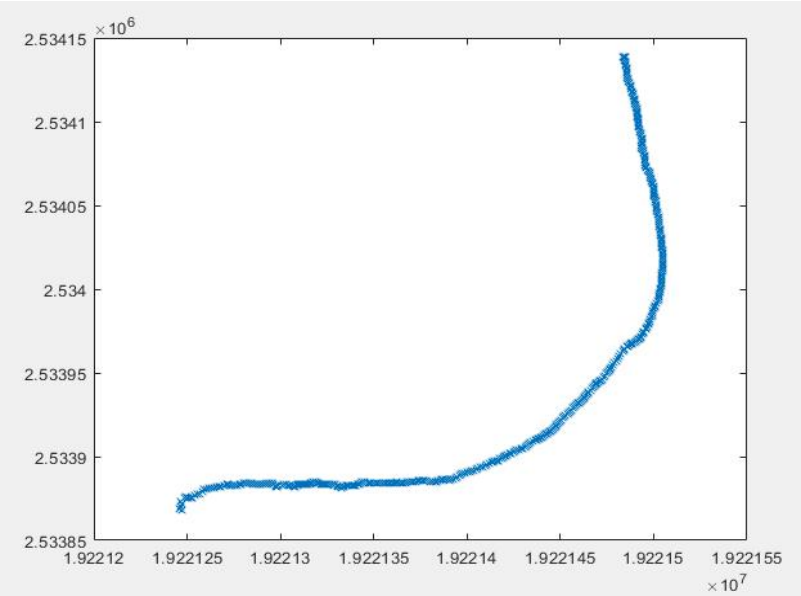

Figure 12: Positioning information in the Gauss plane coordinate system

4.4.2 Unified Visual Coordinate System and Plane Coordinate System

The transformation of the visual coordinate system involves the conversion between four

coordinate systems: the world coordinate system, the camera coordinate system, the image coordinate system, and the pixel coordinate system. The world coordinate system describes the position of the camera and serves as a reference for the position of the target object. The origin can be set according to the design requirements. The camera coordinate system has its origin at the optical center of the camera, with the Z-axis parallel to the camera's optical axis, i.e., the direction in which the camera's lens is pointing. The image coordinate system's units are typically in millimeters, with the origin at the intersection of the image diagonal, i.e., the center of the image. The pixel coordinate system's unit is pixels, with the origin at the top-left corner of the image. The transformation between the pixel coordinate system and the world coordinate system is achieved through the camera's intrinsic and extrinsic parameters, which can be obtained via camera calibration using MATLAB.

The robot's position at time k is obtained by subtracting the combined position error from the position data obtained by the BDS at time k. The combined position error is calculated by subtracting the position data obtained by the BDS at time k-1 from the target point on the navigation line extracted by the vision system at time k-1. The unification of the visual coordinate system and the plane coordinate system is completed through the following steps: First, the data obtained from the Beidou positioning system is converted from the Beidou coordinate system to the Gauss plane coordinate system. In the plane coordinate system, the X-axis is positive toward the north and the Y-axis is positive toward the east, which serves as the reference coordinate system for unifying the two coordinate systems. The robot's coordinates are set as (x_0, y_0)。 The projection of the camera's front center onto the ground is taken as the origin of the visual coordinate system. The positive direction of the x-axis is set along the robot's forward direction, and the y-axis is perpendicular to the x-axis and points to the right. The reference point extracted through the visual algorithm is taken as the target point W, with its coordinates in the visual coordinate system denoted as (x_{w1}, y_{w1})， The coordinates of the target point W in the plane coordinate system are denoted as (x_w, y_w)， As shown in Figure 13, the unification of the visual coordinate system and the plane coordinate system can be completed using the following equation (16), and the coordinates of the target point W in the plane coordinate system can be obtained.

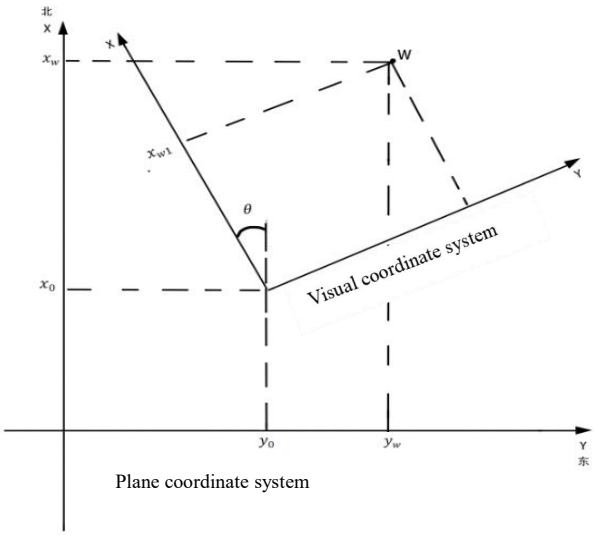

Figure 13. A schematic diagram of the coordinate system

$$\begin{bmatrix} x_w \\ y_w \end{bmatrix} = \begin{bmatrix} \cos\theta & \sin\theta \\ \sin\theta & \cos\theta \end{bmatrix} \begin{bmatrix} x_{w1} \\ y_{w1} \end{bmatrix} + \begin{bmatrix} x_0 \\ y_0 \end{bmatrix} \qquad (16)$$

4.5 Simulation Experiment and Analysis

To verify the effectiveness of the combined navigation algorithm using the visual system and the Beidou system, a semi-physical simulation analysis of the fusion algorithm was conducted. The experimental procedure is as follows: In the Nanning Flower Park, a segment of approximately 20 meters in length was selected. First, the machine vision system was used to extract the navigation line. Then, the RTK environment was set up, and the robot traveled along the navigation line at a speed of 0.5 meters per second. The measured path data was used as the baseline, which was compared with the fusion data. Afterward, the RTK environment was turned off, and the BDS system was used independently. The robot continued to travel along the navigation line at the same speed of 0.5 meters per second, recording data. Finally, the fusion algorithm was applied, and a total of three sets of data were recorded. One set was selected for analysis, and the result is shown in Figure 14.

As seen in Figure 14, the data obtained from the BDS system alone, even after filtering, still shows a significant error compared to the baseline data. However, the positioning data obtained using the fusion algorithm is much closer to the baseline data compared to the positioning data from the single sensor navigation. This indicates that the precision of the navigation system is significantly improved when using the fusion algorithm.

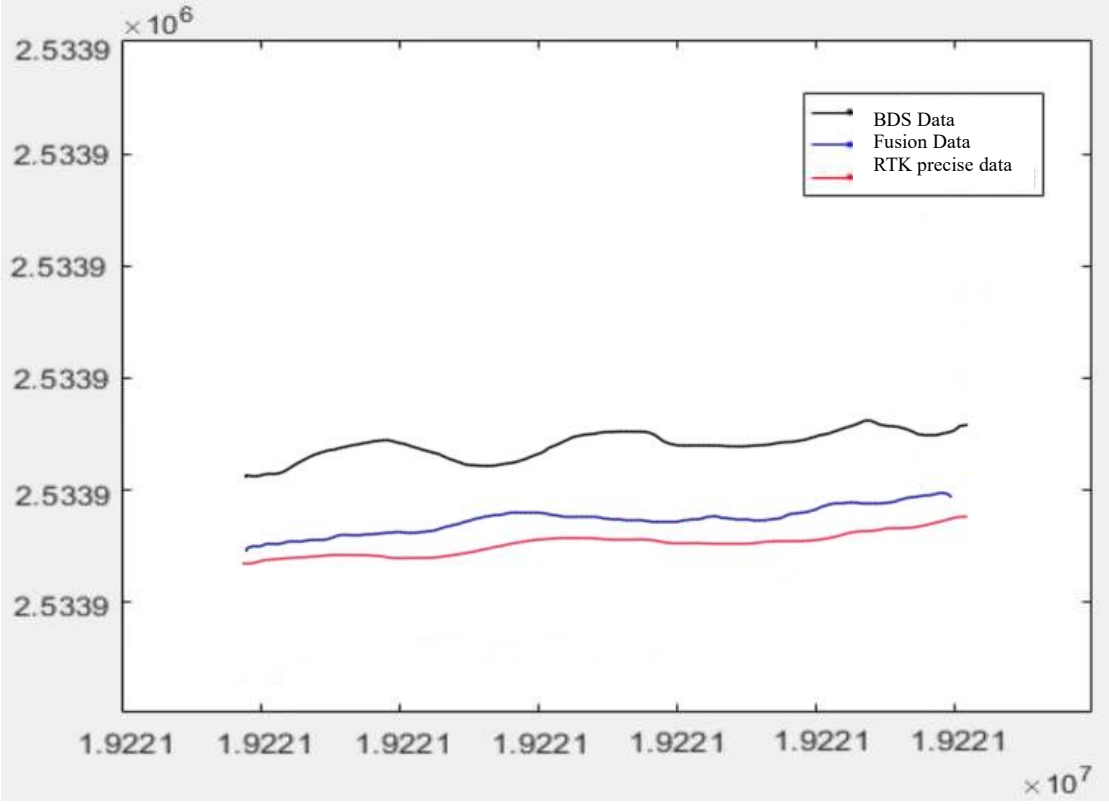

Figure 14: Semi-physical simulation result of the experiment.

5.Conclusion

This study proposed and validated a combined navigation algorithm that integrates the Beidou satellite positioning system with a machine vision system, addressing the limitations of individual sensors and demonstrating significant improvements in navigation accuracy and robustness for garden robots. Experimental results from semi-physical simulations in a real-world environment confirmed that the fusion algorithm achieved higher precision compared to standalone BDS or vision systems, highlighting its potential for practical applications. However, future work should focus on optimizing computational efficiency, enhancing adaptability to diverse and complex environments, and conducting extensive testing over longer distances and varied terrains to further validate the algorithm's performance.

5 References

[1] Wang Hongjuan. Agricultural Machinery Automatic Navigation Technology[J]. Shandong Agricultural Mechanization, 2023, (06): 45-47. DOI: 10.15976/j.cnki.37-1123/s.2023.06.010.

[2] Yuan Kun. Analysis of Precise Positioning Methods for Beidou Satellite Navigation System[J]. Integrated Circuit Applications, 2024, 41(05): 322-323. DOI: 10.19339/j.issn.1674-2583.2024.05.149.

[3] Qian Cheng, Liu Xingde, Chen Daguang. Application Research of Multi-Sensor Information Fusion in Industrial Robots[J]. Electronic Production, 2024, 32(03): 106-109. DOI: 10.16589/j.cnki.cn11-3571/tn.2024.03.009.

[3] Qian Cheng, Liu Xingde, Chen Daguang. Application Research of Multi-Sensor Information Fusion in Industrial Robots[J]. Electronic Production, 2024, 32(03): 106-109. DOI: 10.16589/j.cnki.cn11-3571/tn.2024.03.009.

[5] Liu Siqi. Research on Corn Row and Inter-row Weed Detection Methods Based on Machine Vision in Seedling Stage[D]. Northeast Agricultural University, 2023. DOI: 10.27010/d.cnki.gdbnu.2023.000460.

[6] Li Rong. Research on Data Fusion Technology for Underwater Unmanned Aerial Vehicle Navigation[J]. Information Recording Materials, 2023, 24(12): 129-130+133. DOI: 10.16009/j.cnki.cn13-1295/tq.2023.12.074.

[7] Pei Yongjun, Xu Xiaoxin, Mao Meijuan. High-Precision Positioning Method of Satellite Navigation Based on Kalman Filtering Algorithm[J]. Beijing Surveying and Mapping, 2023, 37(10): 1412-1417. DOI: 10.19580/j.cnki.1007-3000.2023.10.017.

[8] Wan Huan, Ou Yuanzhen, Guan Xianlu, et al. Review of Environmental Perception Technologies for Unmanned Agricultural Machinery[J]. Transactions of the Chinese Society of Agricultural Engineering, 2024, 40(08): 1-18.

[9] Fu Jiahao. Research on Agricultural Machinery Navigation System Based on Beidou and Vision[D]. Anhui University of Science and Technology, 2023. DOI: 10.26918/d.cnki.ghngc.2023.000310.

[10] Wang Jingjin, Li Chengzhi. Development and Innovation of Beidou Satellite Navigation System[J]. Studies in the History of Natural Sciences, 2023, 42(03): 365-376.

[11] Liu Huizhong, You Keshun. Extraction and Feature Representation of Rocking Bed Mineral Belt Boundaries Based on Deep Learning Edge Detection and Hough Transform[J]. Manufacturing Automation, 2023, 45(06): 180-183+188.

[12] Wang Zhongtao. Research on Indoor Positioning Method Based on Data Fusion Technology[J]. Residential Industry, 2020, (03): 72-74.

[13] Jia Nan. Design of GPS System Based on Embedded Linux[J]. China High-tech Enterprises, 2008, (22): 135-136.

[14] Chen Gucang. Construction and Development of Beidou Satellite Navigation System[J]. Satellite Applications, 2023, (06): 8-11.

[15] Wang Junzhou. Research on GNSS-Aided Ground-based Pseudo-satellite Combined Positioning[D]. Hunan University, 2020. DOI: 10.27135/d.cnki.ghudu.2020.004348.

[16] Zhang Ximin, Zhan Haisheng, Yu Qiying. Hough Transform Line Detection Algorithm Based on Voting Constraints[J]. Electronic Design Engineering, 2023, 31(19): 89-93. DOI: 10.14022/j.issn1674-6236.2023.19.019.

[17] Zhang Minghua, Ding Xin, Liu Chibiao. Research on a New Agricultural Pest Trap Monitoring System Based on Binary Image Recognition[J]. Journal of Nanchang University (Natural Science Edition), 2019, 33(01): 74-79.

[18] Chen Jiqing, Qiang Hu, Xu Guanwen, et al. Navigation Line Extraction for Landscape Spraying Robot Based on Hough Transform[J]. Modern Electronic Technology, 2020, 43(20): 183-186. DOI: 10.16652/j.issn.1004-373x.2020.20.046.

[19] Liu Jian, Lu Jiahua, Yang Xinyun, et al. Deformation Analysis of Lambert Projection and Gauss-Krüger Projection in Mid-latitude Areas[J]. Geomatics and Mineral Surveying, 2019, 35(03): 12-14+17. DOI: 10.16864/j.cnki.dkch.2019.0037.

[20] Hou Jinliang. Research on Industrial Robot Trajectory Planning Algorithm Based on Vision Guidance[D]. Shaanxi University of Science and Technology, 2018.

[21] Liu Siqi. Research on Row and Inter-row Weed Detection Method for Maize Crops in the Seedling Stage Based on Machine Vision[D]. Northeast Agricultural University, 2023. DOI: 10.27010/d.cnki.gdbnu.2023.000460.

[22] Yuan Kun. Analysis of Precise Positioning Method of Beidou Satellite Navigation System[J]. Integrated Circuit Applications, 2024, 41(05): 322-323. DOI: 10.19339/j.issn.1674-2583.2024.05.149.

[23] Qian Cheng, Liu Xingde, Chen Daguang. Application Research of Multi-sensor Information Fusion in Industrial Robots[J]. Electronic Production, 2024, 32(03): 106-109. DOI: 10.16589/j.cnki.cn11-3571/tn.2024.03.009.

[24] Wang Jingjin, Li Chengzhi. The Construction History of China's Beidou Satellite Navigation System[J]. Science, 2024, 76(01): 35-39+69.

[25] Wang Hongjuan. Agricultural Machinery Automatic Navigation Technology[J]. Shandong Agricultural Mechanization, 2023, (06): 45-47. DOI: 10.15976/j.cnki.37-1123/s.2023.06.010.

[26] Li Rong. Research on Navigation and Positioning Data Fusion Technology for Underwater Unmanned Vehicles[J]. Information Recording Materials, 2023, 24(12): 129-130+133. DOI: 10.16009/j.cnki.cn13-1295/tq.2023.12.074.

[27] Pei Yongjun, Xu Xiaoxin, Mao Meijuan. Satellite Navigation High-Precision Positioning Method Based on Kalman Filtering Algorithm[J]. Beijing Surveying and Mapping, 2023, 37(10): 1412-1417. DOI: 10.19580/j.cnki.1007-3000.2023.10.017.

[28] Wan Huan, Ou Yuanzhen, Guan Xianlu, et al. Review of Unmanned Agricultural Machinery Operating Environment Perception Technology[J]. Transactions of the Chinese Society

of Agricultural Engineering, 2024, 40(08): 1-18.